



Hassouna, Y. M., Zamani, S., Kafienah, W., & Younes, H. M. (2018). Synthesis, characterization & cytocompatibility of poly (diol-co-tricarballylate) based thermally crosslinked elastomers for drug delivery & tissue engineering applications. *Materials Science and Engineering C*, 93, 254-264.  
<https://doi.org/10.1016/j.msec.2018.07.028>

Peer reviewed version

License (if available):  
CC BY-NC-ND

Link to published version (if available):  
[10.1016/j.msec.2018.07.028](https://doi.org/10.1016/j.msec.2018.07.028)

[Link to publication record in Explore Bristol Research](#)  
PDF-document

This is the accepted author manuscript (AAM). The final published version (version of record) is available online via Elsevier at 10.1016/j.msec.2018.07.028. Please refer to any applicable terms of use of the publisher.

## University of Bristol - Explore Bristol Research

### General rights

This document is made available in accordance with publisher policies. Please cite only the published version using the reference above. Full terms of use are available:  
<http://www.bristol.ac.uk/red/research-policy/pure/user-guides/ebr-terms/>

**Synthesis, Characterization & Cytocompatibility of Poly (diol-co-tricarballylate) Based Thermally Crosslinked Elastomers for Drug Delivery & Tissue Engineering Applications**

Youmna M. Hassouna<sup>a</sup>, Somayeh Zamani<sup>a</sup>, Wael Kafienah<sup>b</sup> and Husam M. Younes<sup>a,c\*</sup>

<sup>a</sup>*Pharmaceutics & Polymeric Drug Delivery Research Laboratory, Department of Pharmaceutical Sciences, College of Pharmacy, Qatar University, PO Box 2713, Doha, Qatar.*

<sup>b</sup>*Cellular and Molecular Medicine, School of Medical Sciences, University of Bristol, Bristol, United Kingdom.*

<sup>c</sup>*Office of Vice President for Research and Graduate Studies, Qatar University, P.O. Box 2713, Doha, Qatar.*

\*Correspondence: H. M. Younes. Tel: +974 485-1949. E-mail: husamy@qu.edu.qa.

## Abstract

The aim of this study was to investigate the synthesis and in vitro characterization of thermoset biodegradable poly (diol-co-tricarballylate) (PDT) elastomeric polymers for the purpose of their use in implantable drug delivery and tissue engineering applications. The synthesis was based on thermal crosslinking technique via a polycondensation reaction of tricarballylic acid with aliphatic diols of varying chain lengths (C6-C12). PDT prepolymers were synthesized at 140°C for 20 minutes. After purification, the prepolymers were molded and kept at 120 °C for 18 hours under vacuum to complete the crosslinking process. PDT prepolymers were characterized by DSC, FT-IR, <sup>1</sup>H-NMR and GPC. The PDT elastomers were also subjected to thermal and structural analysis, as well as sol content, mechanical testing, in vitro degradation and cytocompatibility studies. The mechanical properties and sol content were found to be dependent on synthesis conditions and can be controlled by manipulating the crosslinking density and number of methylene groups in the chain of precursor aliphatic diol. The family of thermally crosslinked PDT biodegradable polyesters were successfully prepared and characterized; besides they have promising use in drug delivery and other biomedical tissue engineering applications.

**Keywords:** Poly (diol-tricarballylate), thermal crosslinking, biodegradable elastomer, cytocompatibility, drug delivery

## 1. Introduction

Polymers possessing rubber-like elasticity, known also as elastomers, have been extensively studied for their use in the design and development of drug delivery systems [1-6] and other tissue engineering applications [7-17]. Elastomers possess many advantages over other synthesized tough polymers. Their mechanical properties can be designed to make them as soft as body tissues; they have the ability to withstand the mechanical challenges upon implantation in a moving part of the body and they can also be designed to possess a three-dimensional structure with uniform degradation pattern which make them well suited for various biomedical applications [6, 18].

Biodegradable elastomers can be classified according to their synthesis and thermo-mechanical properties into either, thermoplastics [8, 9, 12] or thermosets [1, 7, 10]. Thermoplastics possess the advantage of being easy to fabricate, but due to their non-amorphous nature they tend to degrade heterogeneously leading to rapid nonlinear loss of their mechanical properties and subsequently leading to significant deformations in their structure. On the other hand, thermosets are not as easy to fabricate but they outperform thermoplastics with uniform biodegradation, better durability and mechanical properties. This made thermosets as a preferable choice for controlled drug delivery and tissue engineering applications.

Various approaches have been reported in literature to prepare thermoset biodegradable elastomers. Such approaches depended mainly on the chemical and physical nature of the monomers utilized and the chemical reaction involved which included but not restricted to polycondensation [19, 20], polyaddition and the commonly utilized ring opening polymerization [21, 22]. Polyester based thermoset elastomers are among the most common types of elastomers synthesized for drug delivery and tissue engineering applications as they are biodegradable,

biocompatible and easily prepared. Younes et al reported earlier on the synthesis of a star  
68 copolymers of poly (D, L- lactide) (PDLLA) and poly ( $\epsilon$ -Caprolactone) (PCL) followed by  
69 preparation of a set of biodegradable polyester based elastomers by utilizing ring opening  
70 polymerization initiated by glycerol [23]. Another recently reported approach to synthesize  
71 polyester diol based thermoset elastomers, comprised the reaction of aliphatic diols, which  
72 contain free alcoholic hydroxyl groups, with acids that possess free carboxylic acid groups via  
73 polycondensation reactions. Poly (alkylene-tartrate) (PAT), poly (glycerol-sebacate) (PGS) and  
74 poly (diol-citrate) (PDC) were most reported examples of such elastomers prepared. [8, 9, 12,  
75 24]. Tri-carboxylic acids were favored in the preparation of such elastomers as they result in  
76 formation of star like prepolymers which facilitate the synthesis of thermoset elastomers [9, 11,  
77 12, 24].

78 Our research laboratory has previously reported on the fabrication and characterization of  
79 photocrosslinked poly (diol-tricarballoylate) (PDT) based elastomers utilizing a process that  
80 involved either visible light or UV light photopolymerization and a solvent free strategy of drug  
81 loading [6, 16, 18]. The use of these PDT based elastomers in cardiac tissue engineering  
82 applications was also recently reported [17]. Those elastomers were optically transparent,  
83 exhibited controllable mechanical properties, and proved to be amorphous with glass transition  
84 temperatures below physiological body temperature, making them suitable as elastomeric  
85 implants *in vivo*. Nonetheless, despite their numerous advantages, the process of their  
86 fabrication involved several steps of synthesis and purification to remove the traces of  
87 photoinitiators and catalysts to maintain their excellent reported biocompatibility [16, 25-28].

88 We selected tricarballoylic acid (propane-1,2,3-tricarboxylic acid) (TCA) and the aliphatic diols  
89 as building blocks for the fabrication of these elastomers since TCA is one of the simplest  
90 classes of aliphatic acids, it is water soluble, and abundantly present in food products and  
possesses structure

similarity to several biological active compounds such as citric acid and amino acid [29, 30]. On the other hand, aliphatic diols are biocompatible intermediate compounds used in the synthesis of polymeric systems including, polyesters elastomers, coatings, adhesives and polymeric plasticizers and their *in vivo* biocompatibility and clearance was extensively reported [18, 31].

The aim of this report, is to report on the direct and simple preparation of monodispersed amorphous, amorphous biocompatible and biodegradable PDT based elastomers via a polycondensation reaction using catalyst-free thermal crosslinking technique. Various aliphatic diols with tricarballic acid have been prepared and characterized. The prepolymers and elastomers prepared have been characterized for their thermal, structural and mechanical properties. In addition, *in vitro* degradation and long-term cytocompatibility studies were conducted. The physicochemical nature of these prepared elastomers was modified by varying the chain length of the aliphatic diol in their structure. As such, these elastomers can be regarded as viable candidates for drug delivery and other biomedical applications that can offer structural integrity and stability over a clinically required period.

## 2. Materials and Methods

### 2.1 Materials

Tricarballic acid, 1,6-hexanediol, 1, 8-octanediol, 1,10-decanediol, 1,12-dodecanediol, Penicillin -Streptomycin Solution and Dulbecco's Phosphate Buffered Saline were purchased from Sigma-Aldrich Chemie GmbH, Germany. Dichloromethane, LiChrosolv<sup>®</sup> acetone, and acetone-d were purchased from Merck Co., Germany. RPMI ( 1640, Fetal Bovine Serum, L-Glutamine 200mM (100x), 2-Mercaptoethanol (50 mM) and the LIVE/DEAD<sup>®</sup> Viability/Cytotoxicity Kit,

for mammalian cells were purchased from Life Technologies Co., Invitrogen, UK. Lonza Trypsin/EDTA (10x) was purchased from SLS Life Science Co., UK. Vybrant® MTT Cell Proliferation Assay Kit was purchased from ThermoFisher Scientific, Paisley, UK. All chemicals and solvents were used as received without any further purification.

## **2.2 Synthesis of Poly (diol-co-tricarallylate) (PDT) Prepolymers and Elastomers**

TCA was reacted with aliphatic diols of varying chain lengths via a polycondensation reaction. A representative synthesis process of poly (1,10-decanediol-co-tricarallylate) (PDET) is described here. Into a glass ampule, an amount of 8.91 g of 1,10-decanediol (0.051 mole) and 6 g of TCA (0.034 moles) were added and mixed. The mixture was heated at 140 °C for 20 minutes with vortex mixing until complete melting. The reaction was then continued for 2 hours under 10 inHg vacuums at 80 °C to prepare the PDT based prepolymers. The prepolymers were poured either into a glass dog-bone shaped mold or in a glass petri dish and left in the oven at 120 °C for 18 hours under 5 inHg vacuums to complete the crosslinking process.

## **2.3 Thermal Characterization**

The thermal properties of the polymers were characterized using DSC 8000 (Perkin Elmer Co., USA) differential scanning calorimeter (DSC) equipped with the intra-cooling system (Intracooler II). The measurements were carried out at heating rate 10 °C/minute. In order to provide the same thermal history, 10 mg of each sample was heated from room temperature to 150°C and rapidly cooled down to -70°C, then DSC scan was recorded by heating from -70 to 150°C. Thermogravimetric data was obtained using Pyris® 6 TGA (Perkin Elmer Co., USA) at a heating rate of 10 °C/min on 10 mg of a sample. The scan run was recorded from room temperature till 600°C.

## 2.4 Structural Characterization

### 2.4.1 X-ray Diffraction Analysis

The X-ray diffraction analysis (XRD) of the monomers' powders and the crosslinked fabricated elastomers was carried out using X-ray diffractometer (D8 Advance, Bruker Co., Germany) employing CuK $\alpha$  radiation source. A 1° divergence slit was used to analyze between the 2 $\theta$  range 5-40° with a step size of 0.1° and step time of 1 second. The other various components were assigned through auto-fitting in the instrument using the DIFFRAC.EVA<sup>®</sup> software.

### 2.4.2 Fourier Transform-Infrared

Fourier Transform-Infrared (FT-IR) spectra of the prepared PDT based prepolymers and elastomers were obtained at room temperature using Jasco<sup>®</sup> FT/IR-4200 (Jasco Inc., Japan) infrared spectrometer equipped with ATR PRO470-H attenuated total reflection accessory unit, over the wavelength range of 4000–400 cm<sup>-1</sup>. The spectra were collected with a resolution of 4 cm<sup>-1</sup> and a scan number of 32 using a DLA-TGS detector.

### 2.4.3 Proton Nuclear Magnetic Resonance

Proton Nuclear Magnetic Resonance (<sup>1</sup>H-NMR) spectra for the prepared prepolymers were recorded at room temperature on a Bruker Ascend<sup>®</sup> 600 MHz NMR spectrometer (Bruker Co., Germany). The samples were dissolved in deuterated acetone containing 0.1% (v/v) tetramethylsilane) in a 5 mm diameter NMR tubes for analysis. The chemical shifts in parts per million (ppm) for the <sup>1</sup>H-NMR spectra were referenced relative to tetramethylsilane (TMS, 0.00 ppm) as the internal reference.



#### 2.4.4 Gel-permeation Chromatography (GPC)

Molecular weights and molecular weight distributions of the prepared prepolymers were determined using a Viscotek GPCmax VE 2001 gel-permeation chromatography (Viscotek, Malvern, UK) equipped with triple detector array TDA 305 (Light Scattering: RALS 90° angle and LALS 7° angle, Refractive Index and Viscometer). The column configurations consisted of 4 columns connected in series: T6000M (300 x 8 mm), two T1000 (300 x 8 mm) and FIPA (H100-3078). The mobile phase consisted of acetone at a flow rate of 1 ml/min at 35°C. The sample concentration was 20 mg/ml, and the injected volume was 100 µl. Data were collected and handled using OmniSEC® software package.

#### 2.5 Sol Content Measurements

Soxhlet extraction was used in determining the sol content of PDT elastomers with dichloromethane (DCM) as a solvent for 24 hours at 45 °C. Slab samples (20×6×3mm) with weight ( $W_1$ ) were evaluated. The samples were then dried using two filter papers and weighed ( $W_2$ ). After that, the samples were dried in vacuum oven at 55°C and maximum vacuum till obtaining constant weight ( $W_3$ ). Results reported are the mean  $\pm$  SD of triplicate for each elastomeric sample. The sol content and the swelling degree of the prepared elastomers were calculated using the following equations:

$$\text{Sol content (\%)} = (W_1 - W_3) / W_1 \times 100$$

$$\text{Swelling degree (\%)} = (W_2 - W_3) / W_3 \times 100$$

## 2.6 Contact Angle Measurements

The contact angles for fabricated elastomers were determined using a goniometer Drop Shape Analysis System, DSA25, (Krüss GmbH, Hamburg, Germany), equipped with a microsyringe PTFE needle of 0.5 mm diameter. Using the dynamic sessile drop method, a drop of deionized water (10  $\mu$ L) was dispensed, and then the syringe needle was moved down to the surface of the elastomeric films. After dispensing, the drop shape was captured with a digital camera within 5 s, and contact angle, drop diameter were recorded. To determine the contact angle, the drop contour was mathematically described by the Young–Laplace equation using DSA25, and the contact angle was determined as the slope of the contour line at the three-phase contact point. Five measurements were taken for each sample at different sites and were averaged.

## 2.7 Mechanical Properties

Tensile mechanical testing was conducted using Instron tensile 3343 tester with Bluehill® software (Instron Co., USA). The tensile tester was equipped with 1 N load cell. Dog-bone shaped samples of 28 mm in length, 1.5 mm in thickness, 6 mm in width at the narrow section and 15 mm in width at the gripping section. The samples were pulled at a rate of 1.0 mm/sec and elongated to failure at room temperature. Results reported are the mean  $\pm$  SD of triplicate for each elastomeric sample. Differences were evaluated with One-way ANOVA using SPSS software version 20 and a *P* value  $<0.05$  was considered a statistically significant difference. Values were converted to stress-strain and plotted. Young's modulus was calculated from the initial slope of the stress-strain curve. The crosslinking density was calculated according to the theory of rubber elasticity following the equation:  $\rho_x = E / 3RT$ , where  $\rho_x$  represents the number of active network chain segments per unit

volume ( $\text{mol/m}^3$ ),  $E$  represents the Young's modulus in Pascal (Pa),  $R$  is the universal gas constant ( $8.3144 \text{ J/mol K}$ ) and  $T$  is the absolute temperature in kelvin (K).

## 2.8 *In Vitro* Degradation Studies

PDT dog-bone-shaped specimens of known weights ( $W_1$ ), which were 28 mm in length, 3 mm in thickness and 6 mm and 15 mm in width at the narrow and gripping section, respectively, were placed in 40 ml vials each containing 35 ml of 0.1 M phosphate buffered saline (PBS, pH 7.4) and 0.01% sodium azide. The vials were placed in a Julabo SW22 (JULABO Labortechnik GmbH, Seelbach, Germany) shaking water bath at  $37^\circ\text{C}$  and 70 rotations per minute for up to 4 weeks. The buffer was replaced daily to ensure a constant pH of 7.4. After 1, 2, 3 and 4 weeks, the swollen weight ( $W_2$ ) and dried weight ( $W_3$ ) were measured after wiping the surface water with filter paper and after vacuum-drying at  $50^\circ\text{C}$  for 2 days, respectively. The tensile properties of the degraded samples at these intervals were also measured. The results reported as the mean  $\pm$  SD of three measurements.

The water absorption and weight loss calculations were measured as follows:

$$\text{Weight loss (\%)} = W_1 - W_3 / W_1 \times 100$$

$$\text{Water absorption (\%)} = W_2 - W_3 / W_3 \times 100$$

## 2.9 *In Vitro* Cytocompatibility

A murine renal adenocarcinoma cell-line (RENCA-HA) was grown in T75 tissue-culture treated flasks using Roswell Park Memorial Institute Medium (RPMI) supplemented with 10% (v/v) fetal bovine serum, 1% (v/v) L-glutamine, 1% (v/v) penicillin/streptomycin (5000 units), 0.1% (v/v)  $\beta$ -mercaptoethanol and 0.2% (v/v) geneticin (G418) at  $37^\circ\text{C}$  and in a 5%  $\text{CO}_2$ /air atmosphere.

The prepared PDT films were cut into circular discs of 7.6 mm in diameter and 4.3 mm in thickness. The samples were sterilized by soaking in 70% ethanol for 2 minutes followed by washing with PBS. The cells were plated in Falcon® 24-well plates at a density of  $4 \times 10^4$  cells/well in one ml of medium and allowed to attach for 48 hours. Following cells attachment, scaffolds were added to the cells in quadruplicates and assessed after 48 hours of incubation with the cells prior to their staining and measurement. The cells were stained using the LIVE/DEAD® Viability/Cytotoxicity Kit (ETHD-III and Calcein) for mammalian cells. Phase-contrast images and fluorescent images were taken using Leica AF6000 E wide-field microscope (Leica Microsystems, Germany) equipped with a high-resolution Hamamatsu Photonics ORCA C4742-95 CCD camera. Cytotoxicity expressed as relative cell density and cells were assessed visually and qualitatively compared to the control.

PDET scaffolds, as a representative member of the tested PDT based elastomers were subjected to long-term cytocompatibility study over a period of 3 weeks following the same above protocol with the exception that the incubation medium was replaced every 48 hours with a fresh medium. Cells viability was quantified following the MTT 3-(4,5-dimethylthiazol-2-yl)-2,5- diphenyltetrazolium bromide assay protocol as reported by us earlier [18]. Results were recorded as percentage absorbance relative to the incubated control cells only. The cytotoxicity assay results were used to calculate cell viability after incubation with elastomer as follows:

$$\text{Cell viability (\%)} = [A] / [A]_c \times 100$$

Where [A] is the absorbance in a well containing the elastomer sample and [A]<sub>c</sub> is the mean absorbance for control cells. Results reported as the mean  $\pm$  SD from three replicates of the PDET elastomer preparation.

### 3. Results & Discussion

The synthesis of the elastomers (Fig. 1) was achieved through utilization of a polycondensation reaction that was accompanied by a loss of water molecule to form a polyester. The synthesis was carried out at different temperatures according to the stage of the preparation. In the prepolymer preparation stage; TCA was added to the aliphatic diol in a glass ampule and heated at 140 °C for 20 minutes until complete melting of the mix. The use of this relatively high temperature was to ensure complete melting of the acids and the diols, to initiate and facilitate the polycondensation reaction. The prepolymer synthesis continued later at 80 °C and 10 inHg vacuum for two hours.

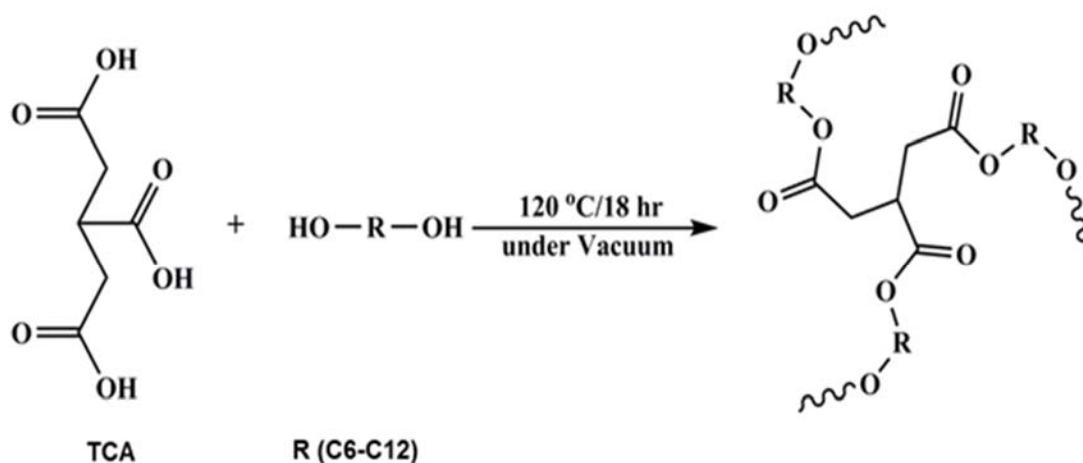


**Fig. 1.** Schematic illustration of the chemical synthesis of PDT based elastomers.

At this stage, the prepolymer (i.e. polymerized but un-crosslinked) obtained was viscous but pourable, transparent, clear and colorless to faint-yellow in color. Those PDT prepolymers were capable to be processed to various shapes by melting or dissolving in organic solvents.

During the elastomer preparation stage, the prepolymers were poured in the desired molds and left in a vacuum oven at 120 °C and 5 inHg vacuums for 18 hours to undergo the thermal crosslinking

process. The molds used were either glass petri dishes to prepare elastomeric films, which were cut afterwards into circular discs, or customized glass dog-bone shaped molds to prepare dog-bone shaped elastomeric specimens, which were subjected to mechanical testing. The prepared crosslinked thermoset PDT based elastomers (Table 1), as with other chemically crosslinked polymers, were neither soluble nor meltable. They were also stretchable, rubbery, and they tend to swell rather than dissolve when placed in organic solvents.

**Table 1**

The monomers used in PDT prepolymers and elastomers synthesis.

Diol used	Acid used	Molar ratio diol: acid	Name	Code of elastomer
1,6-hexanediol	TCA	3:2	Poly(1,6-hexanediol-co-tricarballoylate)	PHT
1,8-octanediol	TCA	3:2	Poly(1,8-octanediol-co-tricarballoylate)	POT
1,10-decanediol	TCA	3:2	Poly(1,10-decanediol-co-tricarballoylate)	PDET
1,12-dodecanediol	TCA	3:2	Poly(1,12-dodecanediol-co-tricarballoylate)	PDDT

### 3.1 Thermal Characterization

#### 3.1.1 Differential Scanning Calorimetry

The thermal analysis of the prepolymers showed that PHT and POT were amorphous while PDET and PDDT were crystalline. The T<sub>g</sub> of the prepared prepolymers are listed in Table 2. After ~~complete~~ the crosslinking process took place, the elastomers converted to the amorphous state with no endothermic peaks detected. As reported, all the prepared elastomers possessed T<sub>g</sub>

temperatures below 37°C which indicated that they will be in their rubbery state at body temperature.

**Table 2**  
Thermal data of PDT prepolymers and elastomers using DSC analysis.

	Prepolymer			Elastomer		
	<i>T<sub>g</sub></i> (°C)	<i>T<sub>m</sub></i> (°C)	$\Delta H$ (J/g)	<i>T<sub>g</sub></i> (°C)	<i>T<sub>m</sub></i> (°C)	$\Delta H$ (J/g)
PHT	-63	-	-	-28	-	-
POT	-59	-	-	-26	-	-
PDET	-41	-8	34	-24	-	-
PDDT	-31	30	46	-10	-	-

The thermal behavior of the PDT prepolymers can be explained as follows: as the number of the methylene groups in the polymer chain increases, the molecular weight also increases, resulting in an increase in both the *T<sub>g</sub>* and the degree of the polymer crystallinity. This is consistent with what was reported earlier concerning the increase in *T<sub>g</sub>* and crystallinity for an aliphatic polyester upon the increase in the number of methylene groups in their backbone chain length [32].

Following crosslinking and the formation of the elastomer, the crystallinity of the prepolymer disappears. This can be explained by the fact that at the prepolymer state, there exists some loose uncrosslinked chains that could have rearranged to form the crystal lattice pattern. Though, after complete crosslinking, to form the elastomers, the network of the loose chains was minimized and disappeared which in turn is reflected on the amorphous state of the elastomer [33]. Thus, the crosslinking suppressed the mobility of the molecular chains and prevented chains rearrangement as a result of which, an obstruction of crystal formation took place [34]. The *T<sub>g</sub>* of the PDT elastomers increased as the elastomer's molecular weight increased. Hence, PHT possessed the lowest *T<sub>g</sub>* at -28 °C, while the PDDT possessed the highest *T<sub>g</sub>* at -10 °C. This is contributed to the

effect of the increase of the molecular weight of the aliphatic polyester on the Tg of the elastomers which are fully crosslinked.

### 3.1.2 Thermogravimetric Analysis

This technique provides complimentary and supplementary characterization information to DSC. The TGA thermograms of PDT elastomers (Fig. 2) demonstrated their stability at high temperatures. Elastomers started to lose their weight at 371 °C and the weight loss increased with the increase in the temperature while maximum degradation took place at 480 °C. These results for PDT were similar to the prepared PDC based elastomers reported by Yang *et. al.* They have observed that the weight loss ranged between 229°C to 274°C [24]. This indicated that TCA was more stable than citric acid as PDT elastomers started their thermal degradation at higher temperatures.

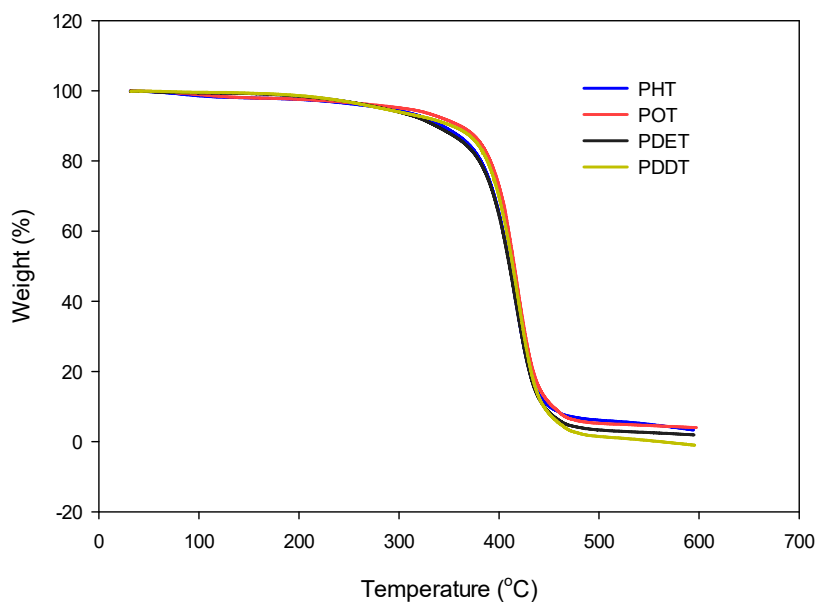


**Fig. 2.** TGA thermograms of PDT elastomers.



## 3.2 Structural Characterization

### 3.2.1 X-ray Diffraction Analysis

The XRD patterns of TCA, (1,6-Hexanediol), (1,8-octanediol), (1,10-decanediol) and (1,12-dodecanediol) powders produced various and distinctive sharp peaks. Conversely, upon crosslinking process and preparation of PHT, POT, PDET and PDDT elastomers, their XRD patterns showed an amorphous-like pattern with no distinctive peaks. This is an indication for the formation of amorphous elastomers and the crosslinking of their monomers. This confirms the results of the DSC, where all the PDT prepared elastomers were found to be amorphous (Fig. 3) with no endothermic peaks.

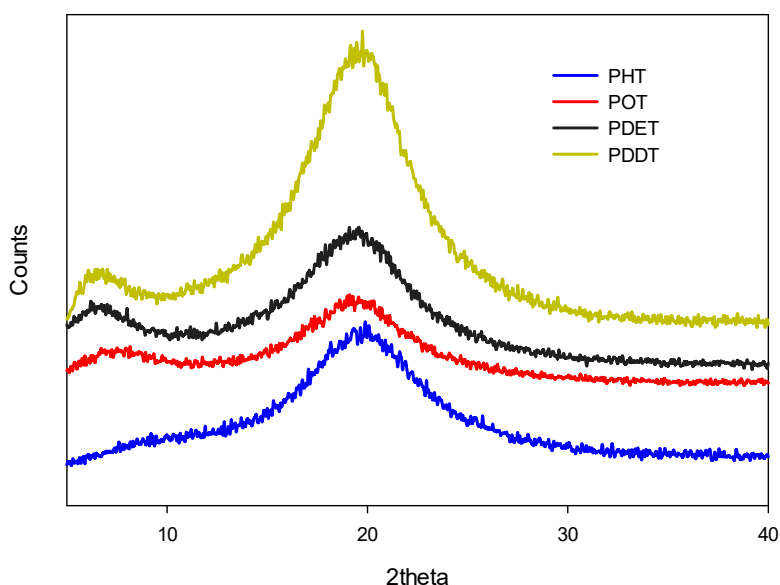


**Fig. 3.** XRD pattern of PDT elastomers.

### 3.2.2 Fourier Transform-Infrared Spectroscopy (FT-IR)

The PDT prepolymers and elastomers with different chain lengths possessed almost the same spectra. The FT-IR spectra of PDET prepolymer and elastomer as a representative example are

shown in Figure 4. The prepolymer possessed three distinctive bands. The first is a broad absorption band at 3600-3400  $\text{cm}^{-1}$  which corresponds to the hydroxyl stretching vibrations for the free OH. The broadening of the band was attributed to the intermolecular hydrogen bond formation. The second absorption bands at about 2938  $\text{cm}^{-1}$  and 2825  $\text{cm}^{-1}$  were attributed to the C-H stretching vibrations of the methylene group. The third absorption band at 1730  $\text{cm}^{-1}$  represented the carbonyl group of the formed ester. The bands at 1300-1000  $\text{cm}^{-1}$  were attributed to C-O stretching vibrations. All these absorptions bands remained the same in the elastomer except for the broad peak at 3600-3400  $\text{cm}^{-1}$  which either disappeared or significantly reduced as a result of the consumption of the OH in the polycondensation reaction to form the ester. These results demonstrated the purity of the structure of the prepared prepolymers and elastomers; as all the peaks in the spectra were corresponding to a certain function group in the samples prepared and there was complete absence of any unexpected peaks in the spectra.

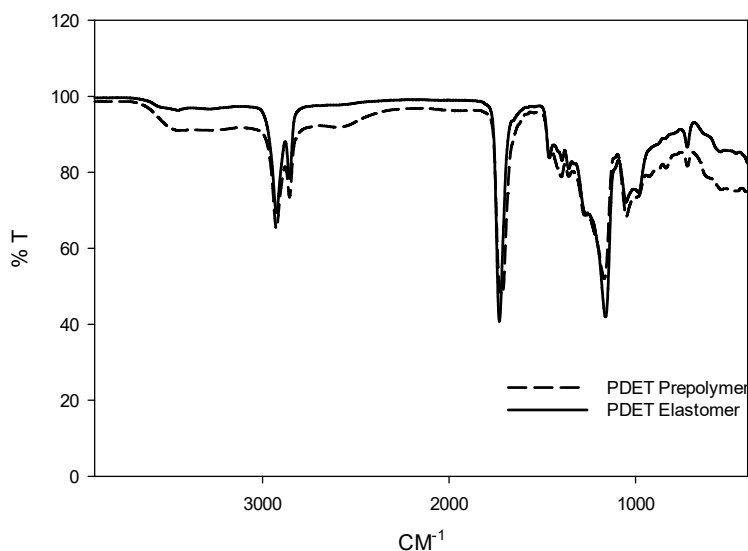


**Fig. 4.** FT-IR spectra of PDET prepolymer and elastomer.

### 3.2.3 Proton Nuclear Magnetic Resonance ( $^1\text{H}$ -NMR)

The  $^1\text{H}$ -NMR spectra (Fig. 5) of PDET prepolymer is used here as a representative example. The peak at 2 ppm represents the solvent used to dissolve the prepolymer (acetone- $d_6$ ). The peak assigned letter (a) that appears at 1.35 ppm was attributed to the protons of the methylene group positioned in the middle of the structure of the 1,10-decanediol. The (b) and (c) (1.5 and 1.65 ppm respectively) represents the protons positioned in the pre-terminal carbon atoms of the diol. The (d) and (e) (2.65 and 2.75 ppm respectively) are the protons located on carbons adjacent to the prochiral center of the TCA. The (f) appears at 3.3 ppm represents the protons of the prochiral center placed just in the middle of the TCA. The (g) and (h) (3.55 and 4.1 ppm respectively) represents the protons of the terminal carbons of the diol which is directly attached to the OH and the ester bond with the acid respectively.

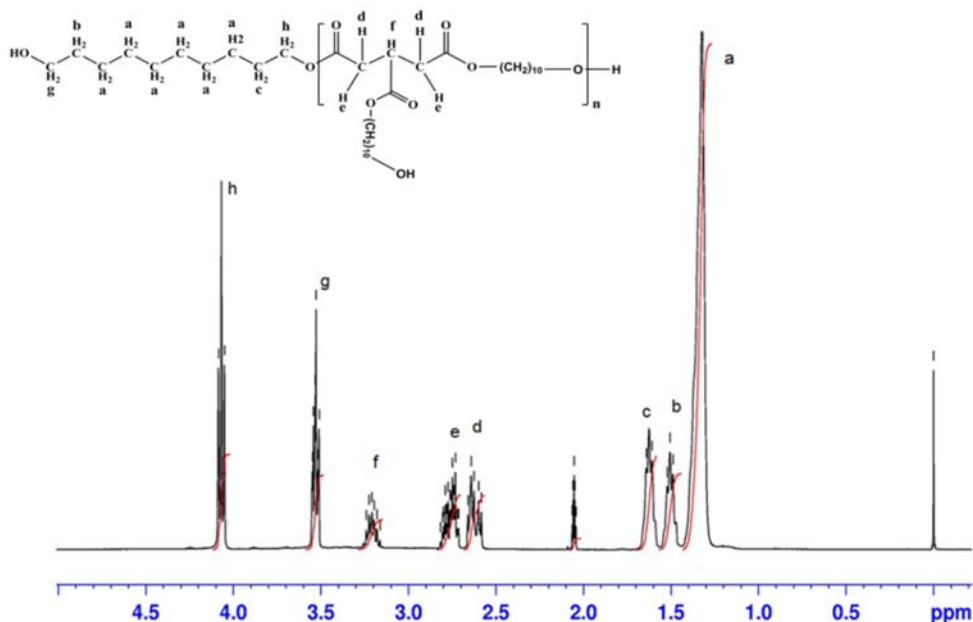


**Fig. 5.**  $^1\text{H}$ -NMR spectra of PDET prepolymer.

### 3.2.4 Gel-permeation Chromatography (GPC)

The molecular weights of the PDT prepolymers as measured *via* GPC are listed in Table 3. As expected, the molecular weights of the prepared prepolymers increased upon increasing the number of the methylene groups in the backbone of the used diol. The GPC analysis also showed that the prepared prepolymers demonstrated narrow distribution of their molecular weights with polydispersity indices approaching unity (1.16 - 1.39). The molecular weights of the prepolymers prepared here were in close alignment with the published GPC data of Younes *et al.* who used the visible light photo-crosslinking technique for the elastomers fabrication [18].

**Table 3**  
GPC results of the PDT prepolymers.

Prepolymer	$M_n$ (g/mol)	$M_w$ (g/mol)	$M_w / M_n$
PHT	835	1049	1.26
POT	934	1131	1.21
PDET	1046	1221	1.16
PDDT	1332	1863	1.39

### 3.3 Sol Content & Swelling Degree

A direct proportional relationship (Fig. 6) between the diol chain lengths to the percentage of sol content and swelling degree was observed. The percentages increased upon increasing the diol chain length from 1,6-hexanediol to 1,12-dodecanediol. The later possessed the highest sol content of 9.5 % and a swelling degree of 215.6%. These results may be attributed to the fact that the crosslinking density decreased upon increasing in the aliphatic diol chain length. As the chain length is a function for the molecular weight; thus, the increase in the molecular weight of the sample, will result in a decrease in the crosslinking which will consequently be translated into an

increase in both the sol content and the elasticity which will be interpreted into the elongation of the elastomers when tested for their mechanical properties.

These results matched what was reported earlier with other elastomeric scaffolds prepared the photocrosslinking methods and using diverse monomers. The photo-crosslinked elastomers using the same monomers as have been reported by our research group; possessed nearly the same range of sol content. The measurements for the photocrosslinked varied from 8-11%. There is a small difference, as the range expressed here in the thermal crosslinked was between 4.5-9.5%. This is due to the fact that the thermal energy produced much greater crosslinked elastomers with higher crosslinking density than those of the photocrosslinked version of the elastomers [15, 16].

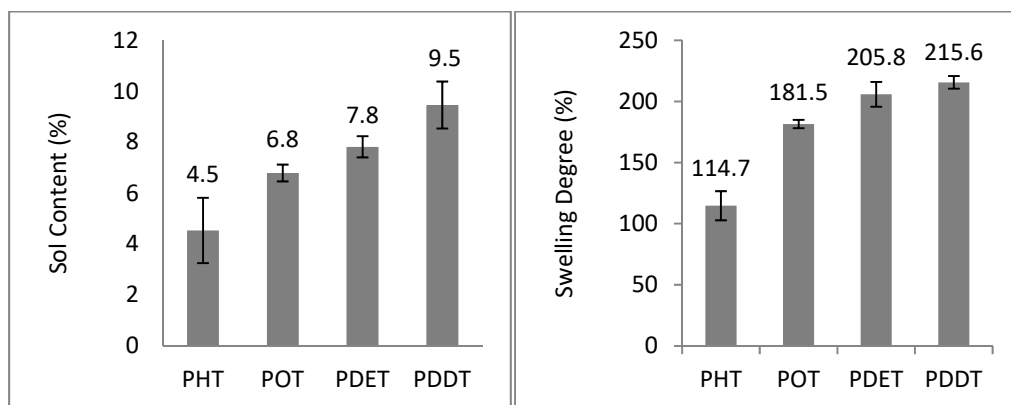


**Fig. 6.** Sol content and swelling degree of PDT elastomers using Soxhlet extraction.

### 3.4 Contact Angle Measurement

The contact angles of the PDT based elastomers increased with increasing the number of methylene groups in the monomers' diol. As reported in Table 4, all the PDT elastomers possessed contact angles below 90° and as such, tend to be more hydrophilic in nature. This has an impact on the elastomers' cytocompatibility, cell attachment, and growth. Many studies proved that cells

attach, spread and prefers growing on moderately hydrophilic substances than on hydrophobic or very hydrophilic ones [18, 35]. PHT with the least number of methylene groups in the diol chain lengths possessed the least contact angle of 72° while PDDT with 12 Carbons in the diol chain length possessed the highest contact angle of 85°. The values of the PDT contact angles followed the same range for different elastomers being prepared using different monomers and crosslinking techniques for tissue engineering and drug delivery applications [36-38].

**Table 4**

The water-in-air contact angles of PDT elastomers.

Scaffold	Contact angle (°)
PHT	72 ± 1.10
POT	76 ± 1.86
PDET	82 ± 1.15
PDDT	85 ± 1.18

### 3.5 Mechanical Properties

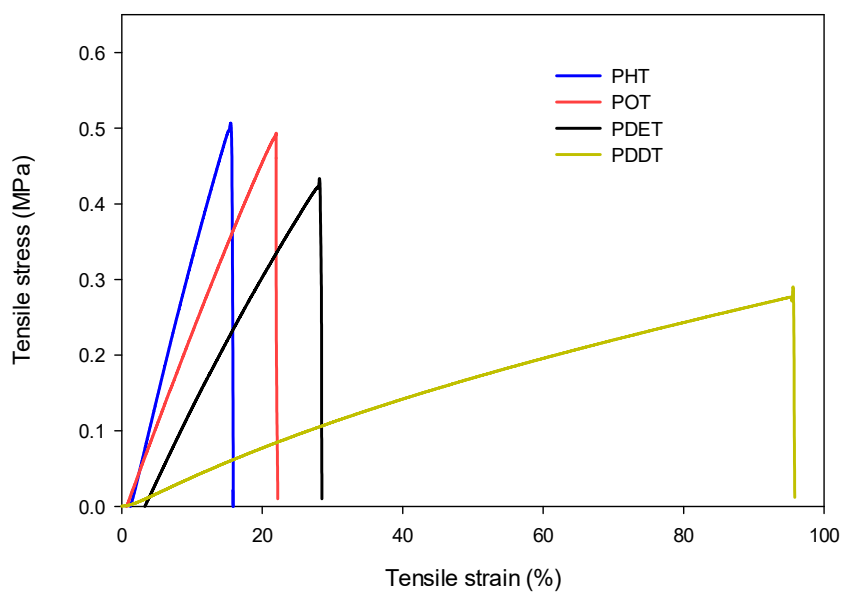
The PDT elastomers were subjected to tensile testing to evaluate the effect of the aliphatic diol chain length on their mechanical properties. As shown in Figure 7, tensile testing of the thermally crosslinked PDT based elastomers produced representative uniaxial tensile-strain curves which are characteristics of typical elastomeric materials. Representative images of PDDT elastomer before and after being tested are shown in Figure 7b. As shown, 100% recovery was obtained for the PDDT elastomer after being stretched to break. Average values of the ultimate tensile stress ( $\sigma$  (MPa)), maximum strain ( $\epsilon$  (%)), the young's modulus ( $E$  (MPa)) and the crosslinking density ( $\rho_c$ ) are summarized in Table 5.

As the chain length of the elastomer decreases, the crosslinking density increases, resulting in a decrease in  $\epsilon$  accompanied by an increase in  $E$ . PHT elastomer showed the highest  $\sigma$  and  $E$  values which was attributed to the fact that PHT possessed the lowest number of methylene groups in the chain of the diol used in their preparation. As the diol chain length decreased, the  $\rho_x$  of the polymer increased, which resulted in the formation of a more crosslinked elastomer that was stiffer and less extensible. On the other hand, increasing the aliphatic diol chain length decreased  $\rho_x$  and, therefore, increased  $\epsilon$  of the elastomer as in PDDT elastomer which possessed the highest chain length of the diol. It also showed a significant difference in its mechanical properties compared to the other elastomers. This could be attributed to the elastomers' crosslinking density. The differences between the crosslinking densities of the other diols were relevantly minimal with increasing of the diol chain length. However, the PDDT was found to be less than that of the PDET by 80%. The sol content of the PDDT elastomer was also higher than the other diols which further proves the effect of the unreacted prepolymer chains within the elastomeric structure which contributes with the long chain length of the PDDT elastomer in having significant results in their mechanical properties.

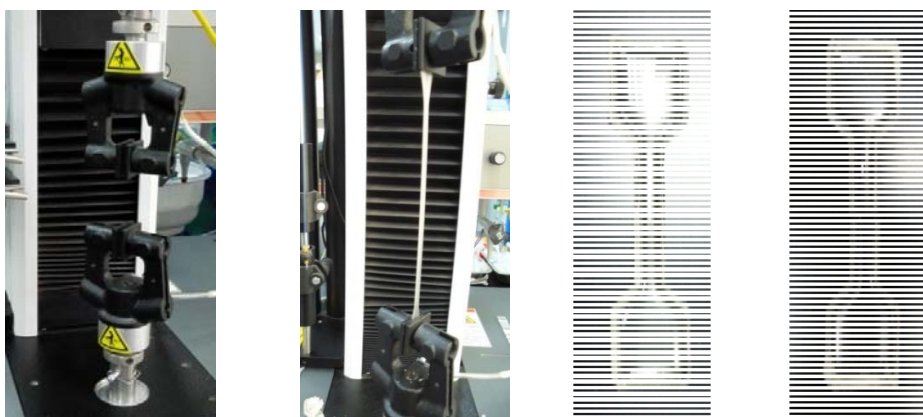
**Table 5**  
Mechanical properties of PDT elastomers.

Elastomer	$\sigma$ (MPa)	$\epsilon$ (%)	$E$ (MPa)	$\rho_x$ (mol/m <sup>3</sup> )
PHT	$0.498 \pm 0.02$	$16.43 \pm 1.11$	$3.57 \pm 0.25^+$	$476.84 \pm 33.39$
POT	$0.454 \pm 0.06$	$20.71 \pm 1.89$	$2.5 \pm 0.46$	$333.92 \pm 61.44$
PDET	$0.424 \pm 0.02$	$28 \pm 3.89$	$1.88 \pm 0.23$	$251.11 \pm 30.72$
PDDT	$0.248 \pm 0.07^*$	$97.72 \pm 12.64^*$	$0.377 \pm 0.07^*$	$50.35 \pm 9.34$

Values are reported as (mean  $\pm$  SD) of triplicates of each sample. The analysis was conducted using One-way ANOVA followed by Tukey's HSD and  $p$  value  $< 0.05$ . (\*) is significant over PHT, POT, and PDET. (+) is significant over POT and PDET.



(a)



(b)

**Fig. 7.** (a) Stress-strain curves of different PDT elastomers. (b) PDDT elastomer shows 100% recovery after being stretched to break.



The obtained mechanical properties were in agreement with reports on other researched thermally-crosslinked elastomers such as those based on star copolymers of DLLA-PCL, PAT, PGS and PDC [8, 9, 12, 23, 24]. For example, in a recent work carried out by Khademhosseini and his group, they observed the decrease in tensile strength and increase in tensile strain of PGS from 0.5 MPa and 38% to less than 0.1 MPa and 98% by tuning the length of polyethylene glycol block attached to the PGS [39].

Many studies have also reported that elastomers' mechanical properties and degradation pattern, as in case of our PDT based elastomers, were found to be heavily dependent on parameters such as polymerization reaction time, reaction temperature, monomers molar ratios and time of curing [9, 24, 31, 37]. For example, in case of PGS, the E was reported to be in the range of 0.056-1.5 MPa, and its elongation at break ranges from 40 to 450 % depending on the synthesis conditions and length of diol chain [31, 37]. On the other hand, poly (diol citrate) (POC), which has raised the most interest of the four reported PDC based elastomers, because of its desirable mechanical properties, was found to have an E ranging from 0.92–16.4 MPa,  $\sigma$  of 6.1 MPa and  $\epsilon$  of 117-265 % [9, 24]. Various studies including this one, which reported on the mechanical and degradation properties of PDT based elastomers have shown comparable mechanical properties to those reported for PGS and PDC elastomers. The E of PDT based elastomers ranged from 0.012-3.5 MPa while  $\epsilon$  ranged from 16- 300% depending on many factors related to synthesis conditions. The above values of E for PDT based elastomers cover those of many soft tissues, such as muscle (0.01–0.5 MPa) [40, 41], skin (0.7–16 MPa)[40, 42] and ligament (0.5–1.5 MPa) [43, 44].

### 3.6 *In Vitro* Degradation

#### 3.6.1 Influence of Chain Length on *in Vitro* Degradation

In order to investigate the influence of chain length on the degradation rate and the changes in the mechanical properties of the elastomer during *in vitro* degradation, four different thermally crosslinked PDT elastomers, based on varying the chain lengths of aliphatic diol were prepared and tested. The water absorption and weight loss (Fig. 8 and Fig. 9) of the elastomers were directly proportional to the chain length of the aliphatic diol used and inversely proportional to the elastomers crosslinking density. PHT elastomer possessed the lowest number of methylene groups in its chain and the highest crosslinking density  $476 \text{ mol/m}^3$ ; demonstrated the lowest weight loss with minimal water uptake rate.

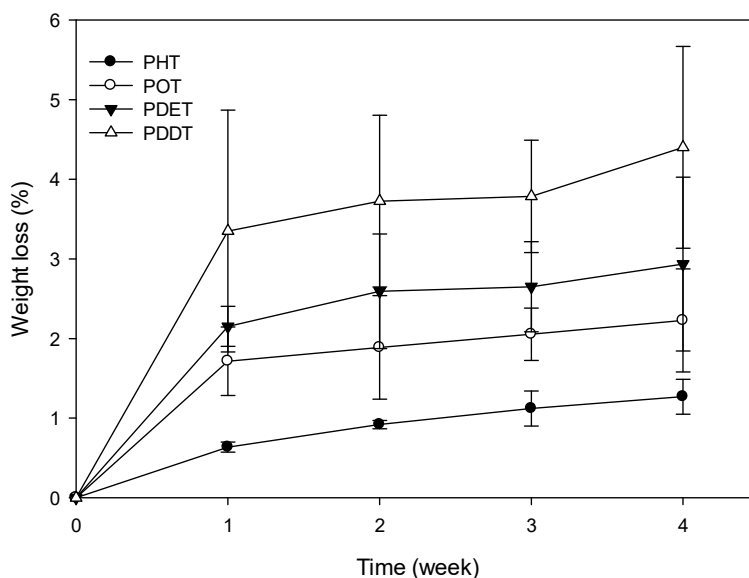


**Fig. 8.** Percentage weight loss versus time of PDT elastomers degradation studies in PBS at 37°C. Error bars represent the standard deviation of the mean of measurements from three samples.

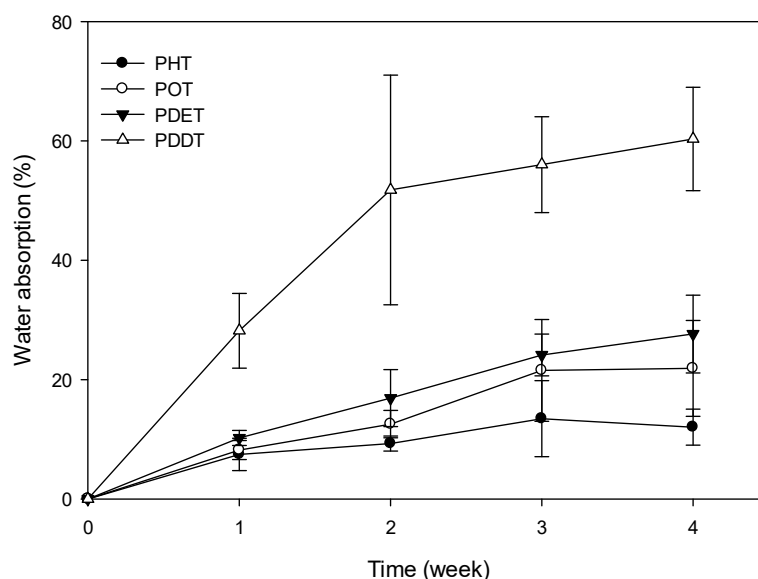


**Fig. 9.** Percentage water absorption versus time of PDT elastomers degradation studies in PBS at 37°C. Error bars represent the standard deviation of the mean of measurements from three samples.

On the other hand, PDDT elastomer, which possessed the highest number of methylene groups in its chain and the lowest crosslinking density ( $50 \text{ mol/m}^3$ ); showed the highest weight loss with maximal water uptake rate. This can be contributed to the high amount of the sol content in the PDDT elastomer which facilitated its degradation. These findings were consistent with PDT elastomers prepared using the photo-crosslinking technique with regards to water diffusion into the bulk of elastomeric polyesters at temperatures above their glass transition [16]. Also, the results are in accordance with the fact that water diffusion and mass loss are inversely proportional to the polymers crosslinking density [45].

### 3.6.2 Degradation Behavior

As with other reported photocured PDT based elastomers [6, 16, 18, 29, 30], some morphological changes of the elastomers' shapes (Fig. 10) were observed during the degradation study. PDDT

was used here as a representative example as the other PDT elastomers behaved similarly. The elastomers retained their dimensions, but they increased in thickness. After the immersion of the elastomeric samples in the PBS; water diffusion and absorption into the elastomer mass took place and resulted in the hydrolysis of the polymer chains. This process wasn't limited to the surface only, but mainly happened to the bulk of the elastomer. The degradation was accelerated by the diffuse out of hydrolysis products from the sol phase of the polymer which further contributed to the formation of oligo carboxylic acids within the polymer mass which autocatalyzed the degradation rate further and increased the hydrophilic character of the polymer due to the formation of free COOH and OH moieties within the elastomer bulk. As such, the elastomers became more susceptible to water absorption. By the end of the fourth week, the samples were swollen and changed from flat shape to bloated convex shape and their surface became smoother and translucent.

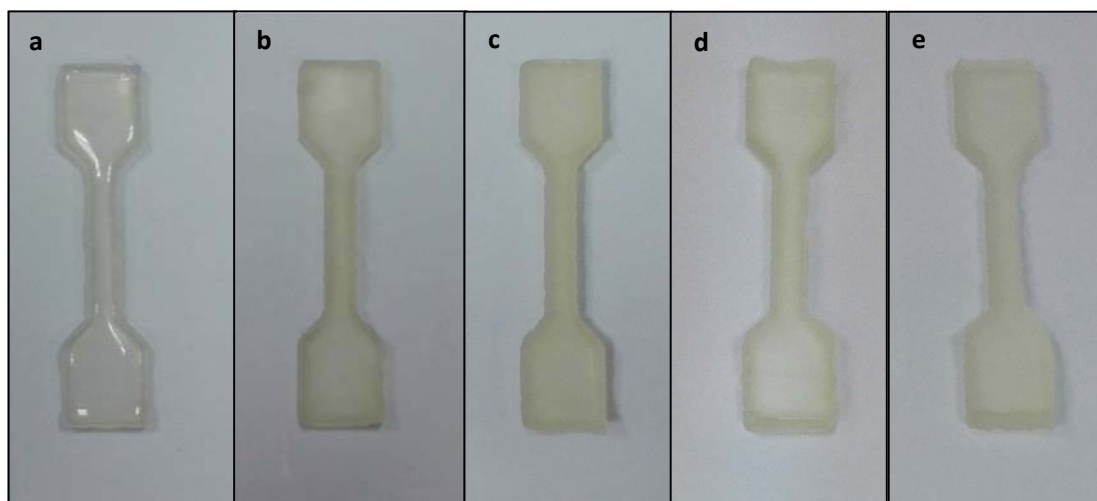


**Fig. 10.** Images of the PDDT elastomers during *in vitro* degradation after (a) 0, (b) 1, (c) 2, (d) 3 and (e) 4 weeks.

### 3.6.3 Changes in the Mechanical Properties during *in Vitro* Degradation

The changes in the mechanical properties (Fig. 11-13) of the elastomers with respect to time during *in vitro* hydrolytic degradation study. Although the elastomers showed a decrease in their mechanical strength with time, they maintained their shape and extensibility over the testing period. Both young's modulus and ultimate tensile stress decreased in a linear fashion with time, indicative of zero-order degradation mechanism. This linear decrease was observed regardless of the network composition, the crosslinking density and the initial young's modulus of the elastomers. The change in the tensile strain (Fig. 13) was less sensitive to the degradation of the PDT elastomers. No significant change in the elongation throughout the four weeks of the *in vitro* degradation study. These results confirmed that the hydrolytic degradation of these elastomers followed a bulk erosion mechanism. It is only with surface erosion degradation pattern that the elastomers can maintain their mechanical properties unchanged [46]. Moreover, young's modulus (Fig. 11) and ultimate tensile stress (Fig. 12) for all the PDT elastomers linearly decreased with time.

Through a linear regression of the zero-order degradation kinetics of the data (Fig. 11 and Fig. 12) using equations (1) and (2), the rate constants were calculated and listed in Table 6.

$$E_t = E_0 - K_E t, \quad (1)$$

$$\sigma_t = \sigma_0 - K_\sigma t. \quad (2)$$

The (t) in the above equations donates to the immersion time (in weeks) in PBS. The values of  $E_0$  and  $\sigma_0$  correspond to the intercepts obtained from extrapolating the zero-order fitted line. While,  $K_E$  and  $K_\sigma$  represents the zero-order degradation constants for young's modulus and the ultimate tensile stress respectively. The decrease in the aliphatic diol chain length in the elastomer was

accompanied by an increase in  $K_E$  and  $K_\sigma$ . As reported in Table 6, PHT which possess the shortest aliphatic in the chain length had  $K_E$  and  $K_\sigma$  of 0.30984 and 0.43763 MPa/week respectively, while PDDT with the longest aliphatic chain length possessed 0.16345 and 0.12655 MPa/week for  $K_E$  and  $K_\sigma$  respectively.

As described earlier in the mechanical testing of the elastomers,  $E$  was depending mainly on the crosslinking density of the elastomers and the ultimate tensile stress depends on the distribution of end to end distances between the crosslinks [45, 46]. As such, lower molecular weight PDT elastomers (shorter chain lengths) demonstrated faster decline in their mechanical strength compared to the higher molecular weight (longer chain lengths) PDT elastomers. These results came with complete agreement with other reported PDT elastomers using photocrosslinking technique, where the degradation rate was inversely proportional to the molecular weight of the elastomers [18]. Thus, the mechanical parameters decrease in a much faster rate as the molecular weight between the crosslinks decreases [16, 46]. By the end of the 4<sup>th</sup> week study period in PBS, the elastomers maintained their original shape with minor degradation.

**Table 6**  
Linear regression coefficients values for PDT elastomers during *in vitro* degradation in PBS (pH 7.4).

Elastomer	$E_0$ (MPa)	$K_E$ (MPa/week)	$\sigma_0$ (MPa)	$K_\sigma$ (MPa/week)
PHT	4.32916	0.30984	2.7198	0.43763
POT	4.01743	0.28078	1.4815	0.17116
PDET	3.42091	0.24859	1.33955	0.16375
PDDT	2.86227	0.16345	1.1462	0.12655

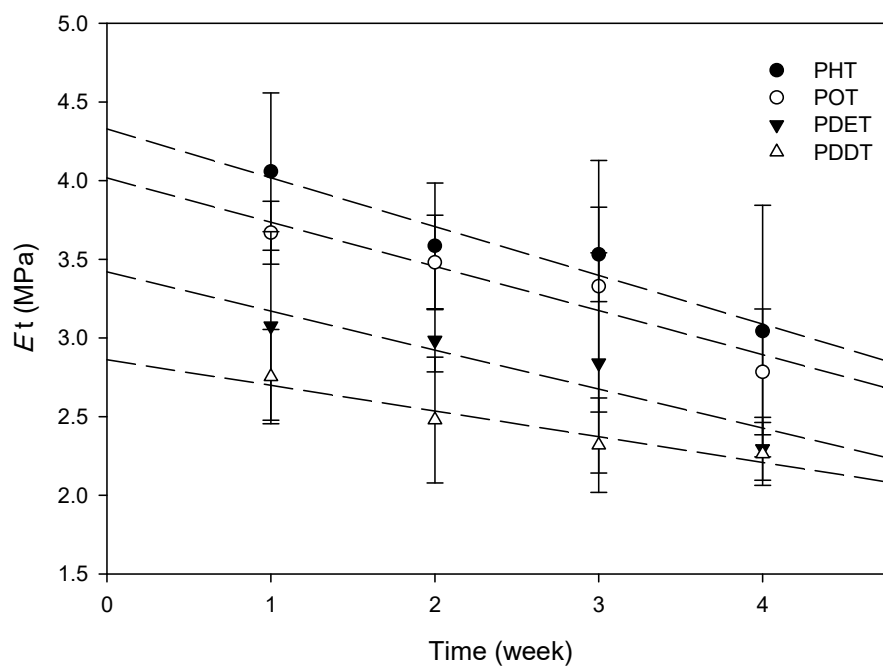


**Fig. 11.** Change in young's modulus of PDT elastomers during degradation in PBS at 37°C. Error bars represent the standard deviation of the mean of measurements from three samples.

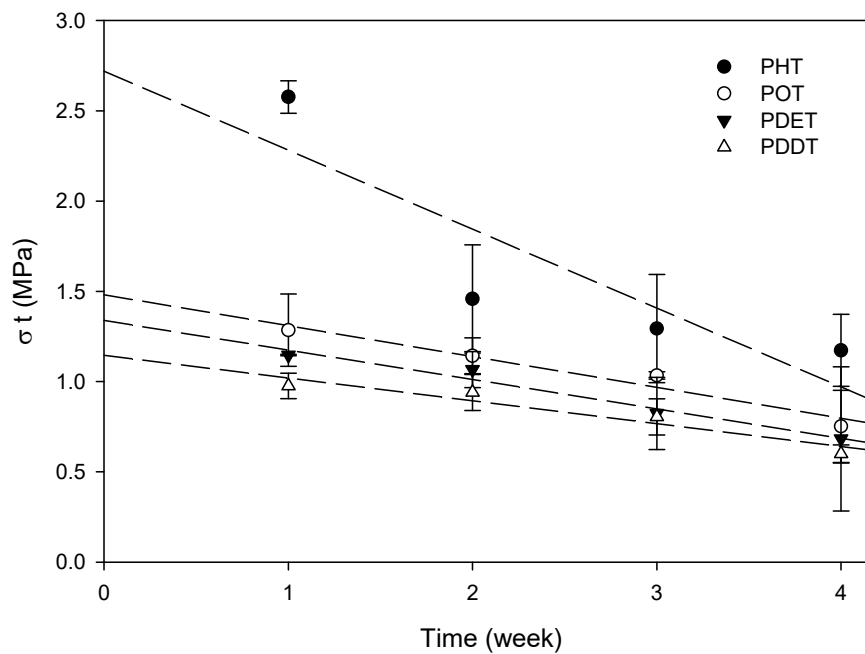


**Fig. 12.** Change in ultimate stress of PDT elastomers during degradation in PBS at 37°C. Error bars represent the standard deviation of the mean of measurements from three samples.

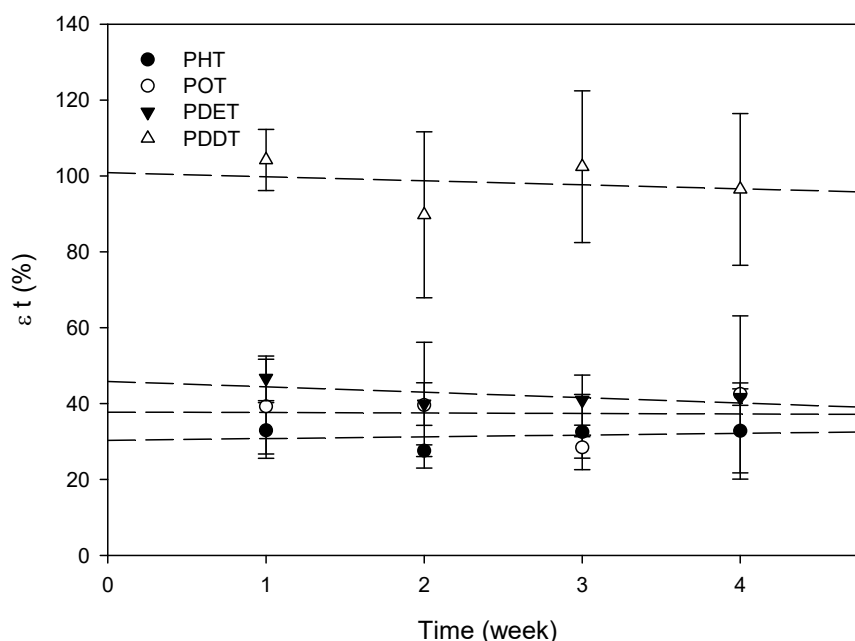


**Fig. 13.** Change in ultimate strain of PDT elastomers during degradation in PBS at 37°C. Error bars represent the standard deviation of the mean of measurements from three samples.

### 3.7 *In Vitro* Cytocompatibility

The different chain lengths of the PDT elastomers were tested for their cytocompatibility using RENCA-HA cells. Firstly, the scaffolds were tested to see if they have any impact on the pH of the media, which has direct effect on the cells proliferation and growth. The PDT elastomeric discs were added in a 24-well plate with 1 ml serum free medium (i.e. no cells were used) and kept overnight in an incubator. The pH of the media was measured using a litmus paper and the change in its color was compared visually to a color pH standard, as well as a control well plate which holds media only. As presented in Table 7, not all the scaffolds showed the same effect on pH of the media. PHT scaffold possessed the least pH indicating more acidity. This may be attributed to the faster degradation of PHT than the other PDT elastomers as have been presented earlier in



Table 6. Upon degradation, the ester bond is hydrolyzed, releasing tricarboxylic acid which is responsible for the drop in the pH of the medium.

**Table 7**

The effect of the different scaffolds prepared on the pH of the media.

Scaffold	pH
Control	8.5
PHT	7
POT	7-7.5
PDET	8
PDDT	8.5

Secondly, RENCA-HA cells were incubated with the PDT elastomers, and then the cells were stained using ETHD-III and Calcein fluorescent dyes. Representative images (Fig. 14) for each PDT scaffolds incubated with the cells, where they were compared to a control well, which possessed the cells only and a negative control well, in which 2 drops of ethanol were added to the control to induce cell death. POT, PDET and PDDT elastomers observed to be more compatible with cells than PHT, possibly due to its faster degradation as reported earlier [18]. The cells were healthy growing, maintaining their spindle shape especially with POT, PDET and PDDT elastomers where the green fluorescence is dominant, which is an indication for living cells that resembled the cells in the control.

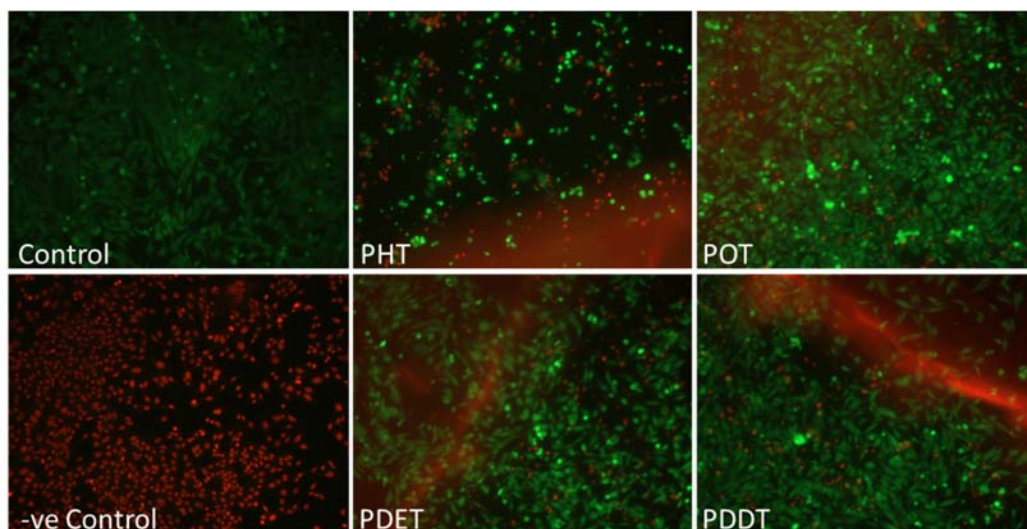


**Fig. 14.** Fluorescent images of RENCA-HA cells incubated with the scaffolds for 48 hours without replacing the media.

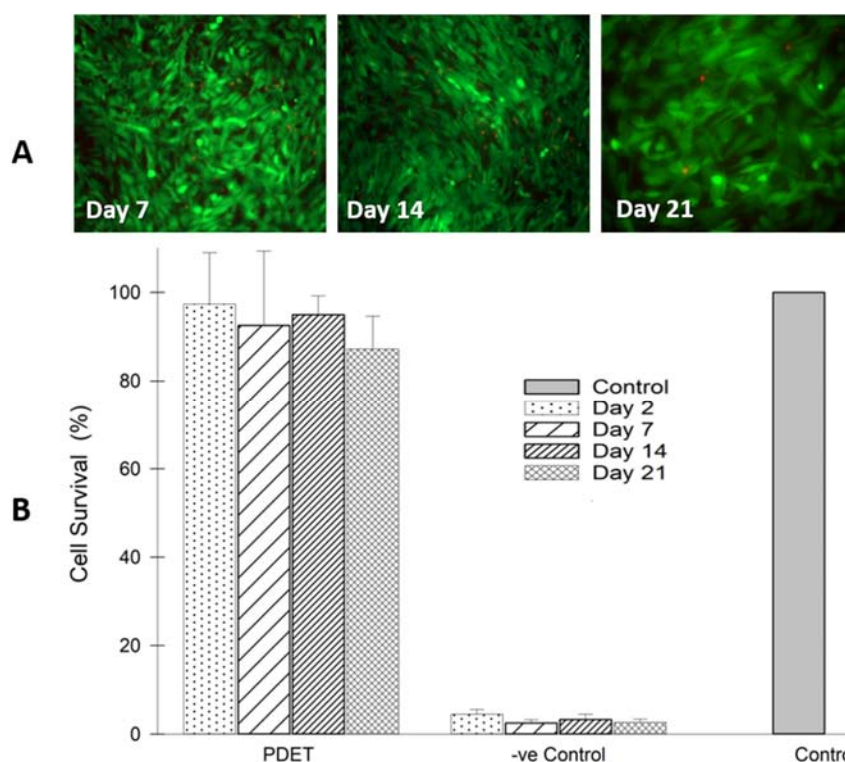


**Fig. 15.** Effect of PDET elastomeric scaffolds on RENCA-HA viability. (A) showing the fluorescent images of cells incubated with the PDET scaffolds over a period of 21 days (25x magnification) and (B) cell viability estimated by MTT assay after 7, 14, and 21 days of PDET elastomer incubation with cells. Results are expressed as the percentage of viable cells compared with controls (mean  $\pm$  SD, n = 3). The significance of the results was determined by comparison with control value using 1-way ANOVA; \*p < 0.05.

Following the long-term cytocompatibility studies on PDET elastomers and as seen in Figure 15a, cells attached were very healthy and maintained their viability over 21 days of incubation. Cells appeared spindle-shaped which is their standard appearance on plastic as undifferentiated cells. There is however at day 21 some change of phenotype (presence of cuboidal cells) suggesting minor differentiation.

The MTT assay results of the PDET elastomers are shown in Figure 15b. The differences in mitochondrial function associated with PDET elastomer were expressed as a percentage relative to the control cells (set at 100%), where higher absorbance values indicated increased metabolic activity of viable cells. The exposure of the cells to the PDET elastomer degradation products did not cause any significant effect on the high metabolic rate. This observation confirmed the biocompatible nature of these elastomers. The above results are in full alignment with the *in vivo* biocompatibility studies in rats conducted on various PDT photocrosslinked based elastomers which exhibited better *in vivo* biocompatibility than PLGA, evidenced by mild acute inflammatory reaction and less fibrous capsules of chronic inflammatory response [18].

## 4. Conclusion

We have reported on the successful syntheses and characterization of different biodegradable PDT elastomers using thermal crosslinking. The elastomers proved to be biocompatible with linear and homogenous degradation. The elastomers can be designed with different crosslinking density and degradation time which make them easily tailored to achieve the desired implantation and drug release rates in the design of controlled drug delivery systems and other biomedical and tissue engineering applications. Full long term *in vivo* biocompatibility and degradation studies in animal

model are needed to further report on the actual immune response and degradation behavior of various fabricated versions of the PDT thermally crosslinked elastomers.

## Acknowledgments

This project was made possible by NPRP grant # NPRP 09 - 969 - 3 – 251 from Qatar National Research Funds (a member of Qatar Foundation) through its National Priorities Research Program granted to Dr. H. Younes (Lead PI) and Dr. Wael Kafienah (PI). The statements made herein are solely the responsibility of the authors.

## Authors Contributions

Ms. Youmna M. Hassouna, the MSc student and Dr. Somayeh Zamani (Postdoc) performed the research experiments, analysis and collected data. Dr. Wael Kafienah guided and helped Youmna Hassouna in performing the *in vitro* cytocompatibility studies. Dr. Husam M. Younes designed the research question and project, designed the performed experiments, analyzed data and wrote the final manuscript.

## References

- [1] J.P. Bruggeman, C.J. Bettinger, R. Langer, J Biomed Mater Res A, 95 (2010) 92-104.
- [2] F. Gu, H.M. Younes, A.O.S. El-Kadi, R.J. Neufeld, B.G. Amsden, Journal of controlled release : official journal of the Controlled Release Society, 102 (2005) 607-617.
- [3] T. Yoshii, A.E. Hafeman, J.S. Nyman, J.M. Esparza, K. Shinomiya, D.M. Spengler, G.R. Mundy, G.E. Gutierrez, S.A. Guelcher, Tissue Eng Part A, 16 (2010) 2369-2379.
- [4] J. Guan, J.J. Stankus, W.R. Wagner, J Control Release, 120 (2007) 70-78.
- [5] S.I. Jeong, B.S. Kim, S.W. Kang, J.H. Kwon, Y.M. Lee, S.H. Kim, Y.H. Kim, Biomaterials, 25 (2004) 5939-5946.
- [6] M.A. Shaker, H.M. Younes, Ther. Deliv, 1 (2010) 37-50.
- [7] I.S. Tobias, H. Lee, J. Engelmayr, D. Macaya, C.J. Bettinger, M.J. Cima, Journal of Controlled Release, 146 (2010) 356-362.

645 [8] A. Borzacchiello, L. Ambrosio, L. Nicolais, S.J. Huang, *Journal of Bioactive and Compatible Polymers*,  
646 SAGE Publications Ltd STM, 2000, pp. 60-71.

647 [9] Y. Wang, G.A. Ameer, B.J. Sheppard, R. Langer, *Nat Biotech*, 20 (2002) 602-606.

648 [10] H. El-Laboudy, M.A. Shaker, H.M. Younes, *Soft Materials*, Taylor & Francis, 2011, pp. 409-428.

649 [11] L. Lijuan, D. Tao, S. Rui, L. Quanyong, Z. Liqun, C. Dafu, T. Wei, *J Polymer Degradation and Stability*,  
650 92 (2007) 389-396.

651 [12] J.P. Bruggeman, B.J. de Bruin, C.J. Bettinger, R. Langer, *Biomaterials*, 29 (2008) 4726-4735.

652 [13] C.J. Bettinger, J.P. Bruggeman, J.T. Borenstein, R.S. Langer, *Biomaterials*, 29 (2008) 2315-2325.

653 [14] J.L. Ifkovits, R.F. Padera, J.A. Burdick, *Biomed Mater*, 3 (2008) 034104.

654 [15] H.M. Younes, US Patent No. 9422396B2 (2016).

655 [16] M.A. Shaker, J.J. Dore, H.M. Younes, *J Biomater. Sci. Polym Ed*, 21 (2010) 507-528.

656 [17] H. Ismail, S. Zamani, M. Elrayess, W. Kafienah, H. Younes, *Polymers* 2018, Vol. 10, Page 455, 10 (2018)  
657 455-455.

658 [18] M.A. Shaker, N. Daneshtalab, J.J.E. Doré, H.M. Younes, *Journal of Bioactive and Compatible Polymers*,  
659 27 (2012) 78-94.

660 [19] I. Miller, J. Zimmerman, *Condensation Polymerization and Polymerization Mechanisms*, Applied  
661 Polymer Science, American Chemical Society, 1985, pp. 159-173.

662 [20] P.J. Flory, *Chemical Reviews*, American Chemical Society, 1946, pp. 137-197.

663 [21] J.P. Pascault, *Thermosetting polymers*, Marcel Dekker, New York, 2002.

664 [22] D. Braun, *Polymer synthesis theory and practice ; fundamentals, methods, experiments*, Springer,  
665 2013.

666 [23] H.M. Younes, E. Bravo-Grimaldo, B.G. Amsden, *Biomaterials*, 25 (2004) 5261-5269.

667 [24] J. Yang, A.R. Webb, G.A. Ameer, *Advanced Materials*, 16 (2004) 511-516.

668 [25] J.P. Fouassier, X. Allonas, *Basics and applications of photopolymerization reactions*. vol. 3, vol. 3,,  
669 Research Signpost, Kerala, India, 2010.

670 [26] R.F. Storey, S.C. Warren, C.J. Allison, A.D. Puckett, *Polymer*, 38 (1997) 6295-6301.

671 [27] Y. Liu, K. Yao, X. Chen, J. Wang, Z. Wang, H.J. Ploehn, C. Wang, F. Chu, C. Tang, *Polymer Chemistry*, 5  
672 (2014) 3170-3181.

673 [28] G. Fangyuan, Z. Wei, P. Xiaohong, S. Xia, Y. Qinying, L. Hanbing, Y. Junxian, Y. Gensheng, *Journal of*  
674 *Bioactive and Compatible Polymers*, SAGE Publications Ltd STM, 2016, pp. 178-195.

675 [29] S.H.E. Abdel-Sattar, *Current Organic Chemistry*, 8 (2004) 1405-1423.

676 [30] W.M. Cumming, I. Vance Hopper, T. Sherlock Wheele, *Systematic organic chemistry: Modern*  
677 *methods of preparation and estimation*. , 2nd edition ed., Constable & Co, London, 1926.

678 [31] Q. Chen, S. Liang, G.A. Thouas, *Progress in Polymer Science*, 38 (2013) 584-671.

679 [32] R. Hill, E.E. Walker, *Journal of Polymer Science*, 3 (1948) 609-630.

680 [33] H. Miyasako, K. Yamamoto, A. Nakao, T. Aoyagi, *Macromol. Biosci*, 7 (2007) 76-83.

681 [34] H. Miyasako, K. Yamamoto, T. Aoyagi, *Polym. J*, 40 (2008) 806-812.

682 [35] K. Webb, V. Hlady, P.A. Tresco, *J Biomed. Mater. Res*, 41 (1998) 422-430.

683 [36] C. Fidkowski, M.R. Kaazempur-Mofrad, J. Borenstein, J.P. Vacanti, R. Langer, Y. Wang, *Tissue Eng*, 11  
684 (2005) 302-309.

685 [37] L.H. Chan-Chan, C. Tkaczyk, R.F. Vargas-Coronado, J.M. Cervantes-Uc, M. Tabrizian, J.V. Cauich-  
686 Rodriguez, *J Mater. Sci. Mater. Med*, 24 (2013) 1733-1744.

687 [38] V. Thomas, J. Muthu, *J Mater Sci Mater Med*, 19 (2008) 2721-2733.

688 [39] A. Patel, A.K. Gaharwar, G. Iviglia, H. Zhang, S. Mukundan, S.M. Mihaila, D. Demarchi, A.  
689 Khademhosseini, *Biomaterials*, 34 (2013) 3970-3983.

690 [40] Y.C. Fung, Springer-Verlag, New York :, 1993.

691 [41] M.A. Meyers, P.-Y. Chen, A.Y.-M. Lin, Y. Seki, *Progress in Materials Science*, 53 (2008) 1-206.

- 692 [42] P.Y. Chen, A.Y.M. Lin, Y.S. Lin, Y. Seki, A.G. Stokes, J. Peyras, E.A. Olevsky, M.A. Meyers, J. McKittrick,  
693 Journal of the Mechanical Behavior of Biomedical Materials, 1 (2008) 208-226.  
694 [43] K. Komatsu, Journal of Dental Biomechanics, 2010 (2010) 502318.  
695 [44] J.D. Lin, H. Özcoban, J. Greene, A.T. Jang, S. Djomehri, K. Fahey, L. Hunter, G.A. Schneider, S.P. Ho,  
696 Journal of biomechanics, 46 (2013) 443-449.  
697 [45] J.M. Halpern, R. Urbanski, A.K. Weinstock, D.F. Iwig, R.T. Mathers, H.A. von Recum, Journal of  
698 Biomedical Materials Research Part A, 102 (2014) 1467-1477.  
699 [46] J.A. Tamada, R. Langer, Proc. Natl. Acad. Sci U. S. A, 90 (1993) 552-556.

700